Supporting Information

Biomimetic *O*-Demethylation at a Copper(II) Center with Imine Ligand: A Structural and Computational Study

Daria Nowicka,[*a] Karol Garbaczewski,[a] Giuseppe Consiglio,[b] Giuseppe Forte,[c] Maciej Kubicki,[a] Teresa Łuczak,[a] Violetta Patroniak [a] and Adam Gorczyński [*a]

[a] Adam Mickiewicz University in Poznań, Faculty of Chemistry, Uniwersytetu Poznańskiego 8, 61-614 Poznań, Poland

[b] Department of Chemical Science University of Catania, Via S. Sofia 64, 95125, Italy

[c] Department of Drug Science and Health University of Catania, Via S. Sofia 64, 95125, Italy

[*] Correspondence: d.nowicka@amu.edu.pl; adam.gorczynski@amu.edu.pl

Table of contents for Supporting Information

1. Synthesis of ligands L1 – L3

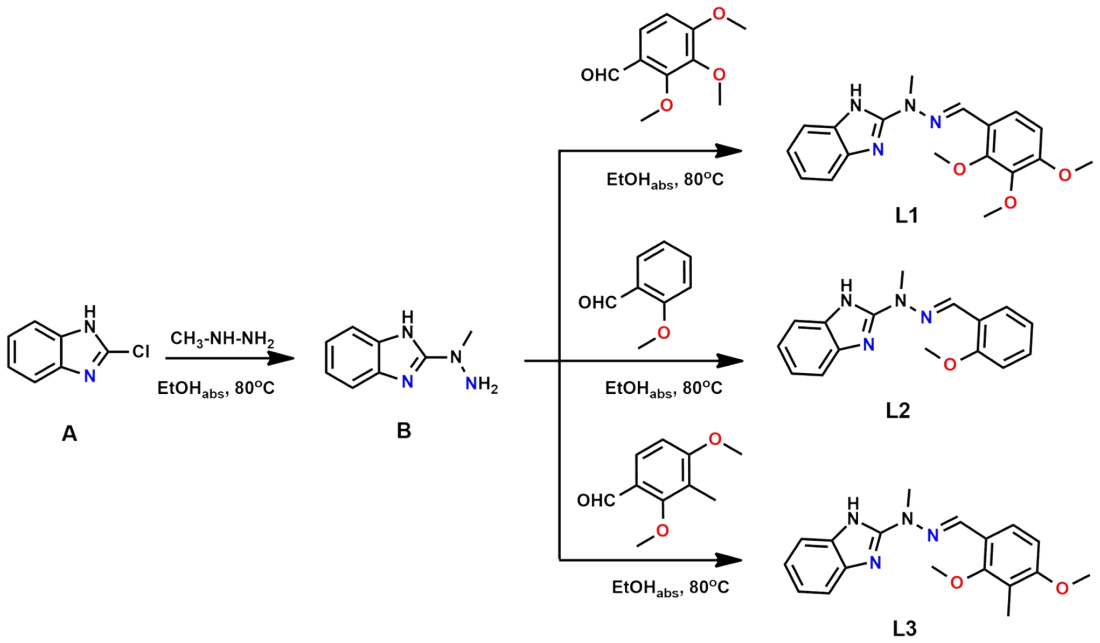

Scheme S1. Scheme of **L1** [$C_{18}H_{20}N_4O_3$], **L2** [$C_{16}H_{16}N_4O$] and **L3** [$C_{18}H_{20}N_4O_2$] ligands synthesis.

2. Synthetic procedure for complexes C4 – C6

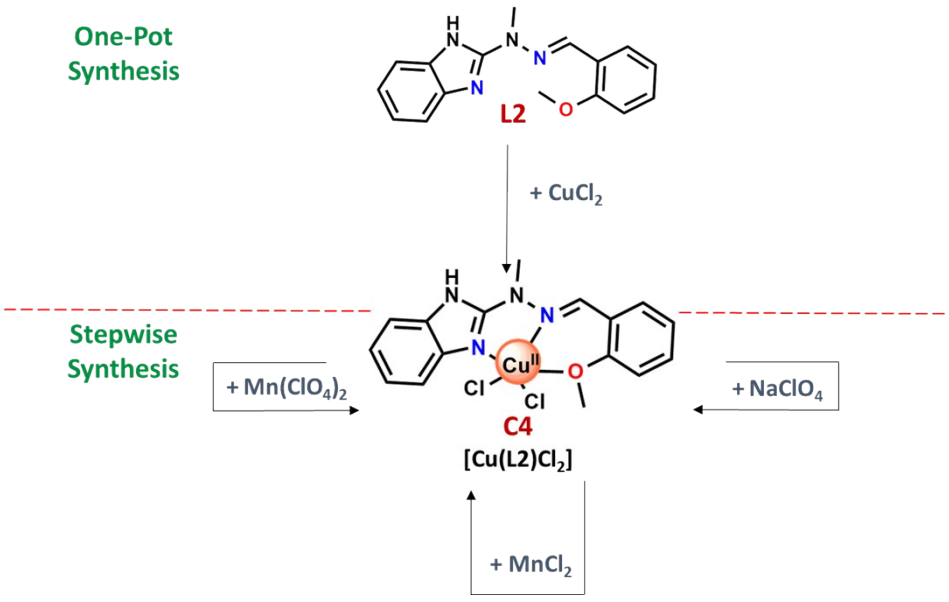

Scheme S2. Schematic representation of the synthetic procedure for Cu(II) complex **C4** based on stepwise and one-pot synthesis. Please note that the replacement of Cu^{2+} by Mn^{2+} or Na^{+} is not favorable either thermodynamically or kinetically. Therefore, the metal center of the complex remains copper, and the use of various perchlorate salts serves only as a source of ClO_4^- anions, not as metal precursors.

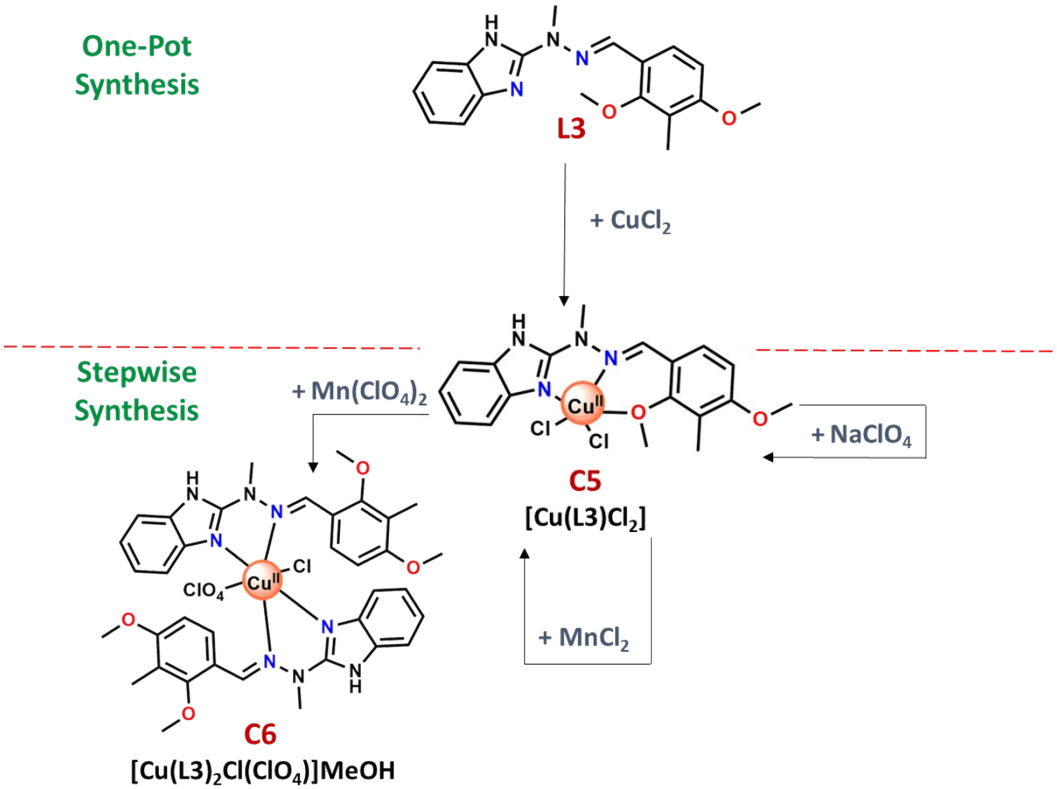

Scheme S3. Schematic representation of the synthetic procedure for Cu(II) complexes **C5** and **C6** based on stepwise and one-pot synthesis. Please note that the replacement of Cu^{2+} by Mn^{2+} or Na^{+} is not favorable either thermodynamically or kinetically. Therefore, the metal center of the complex remains copper, and the use of various perchlorate salts serves only as a source of ClO_4^- anions, not as metal precursors.

3. NMR spectra of ligands L1 – L3

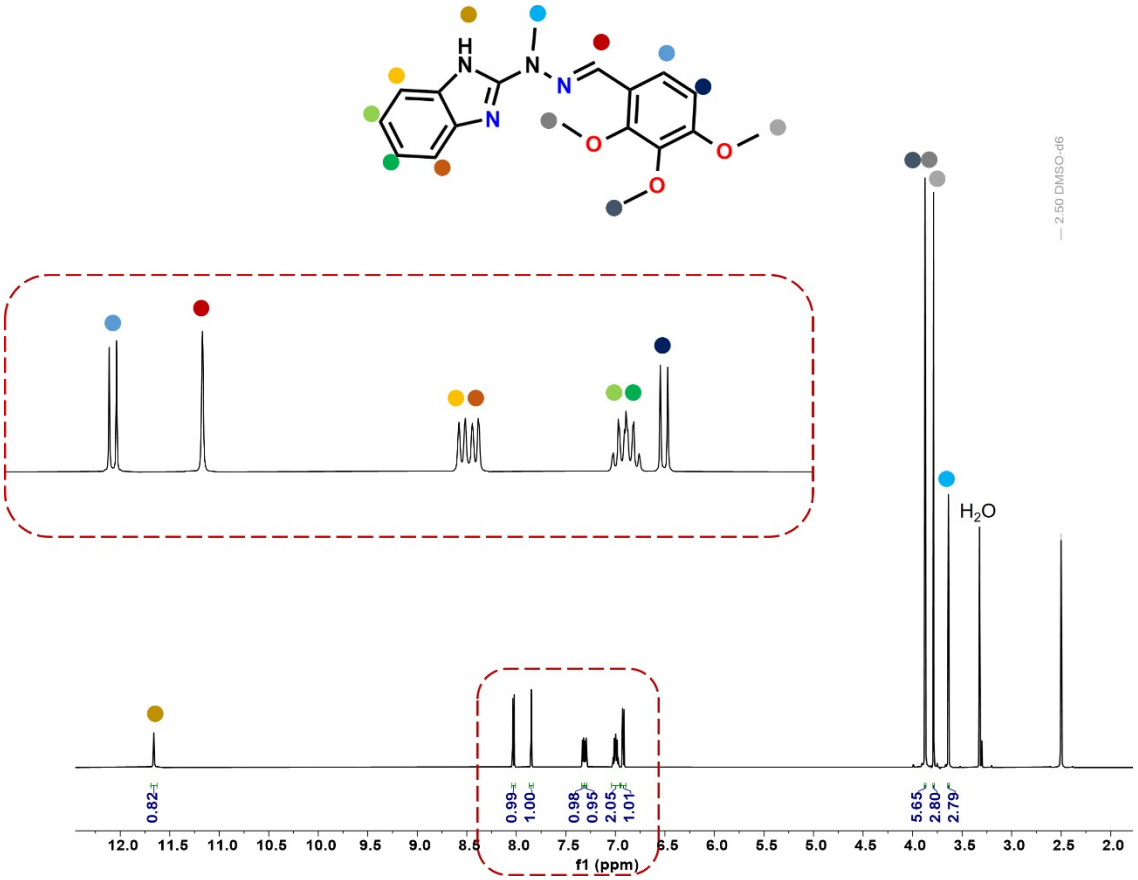

Fig. S1. ^{1}H NMR spectrum for ligand **L1** measured in $(CD_3)_2SO$.

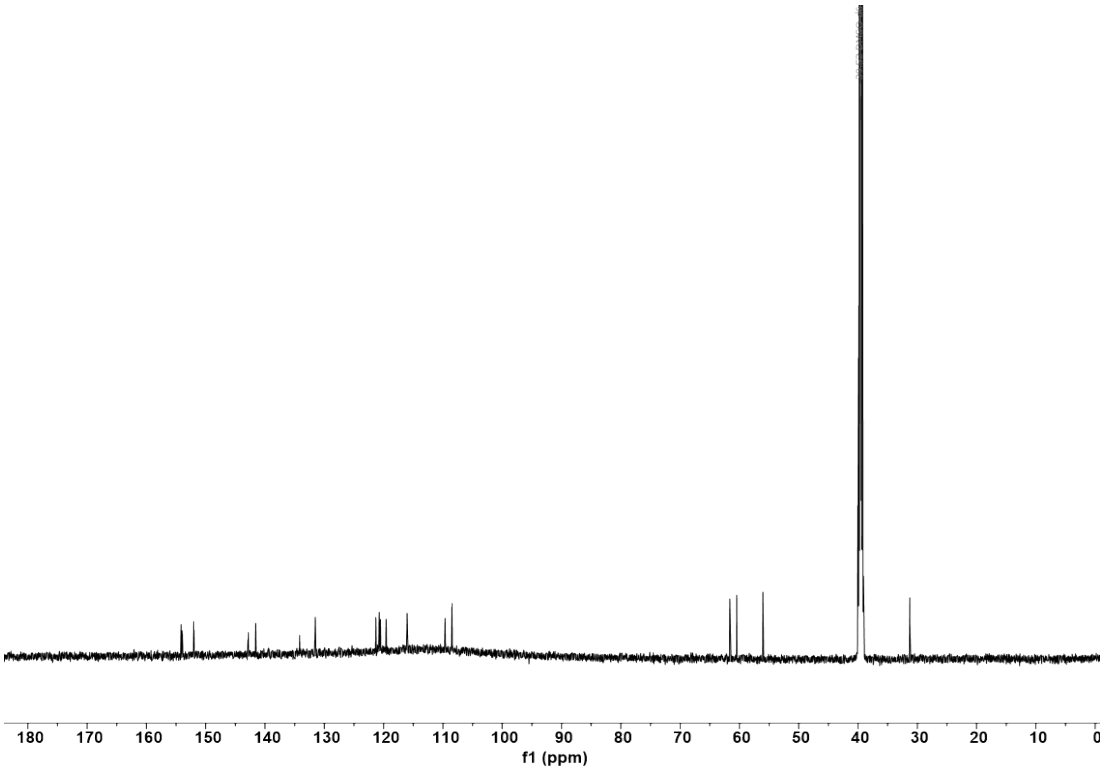

Fig. S2. ^{13}C NMR spectrum for ligand **L1** measured in $(CD_3)_2SO$.

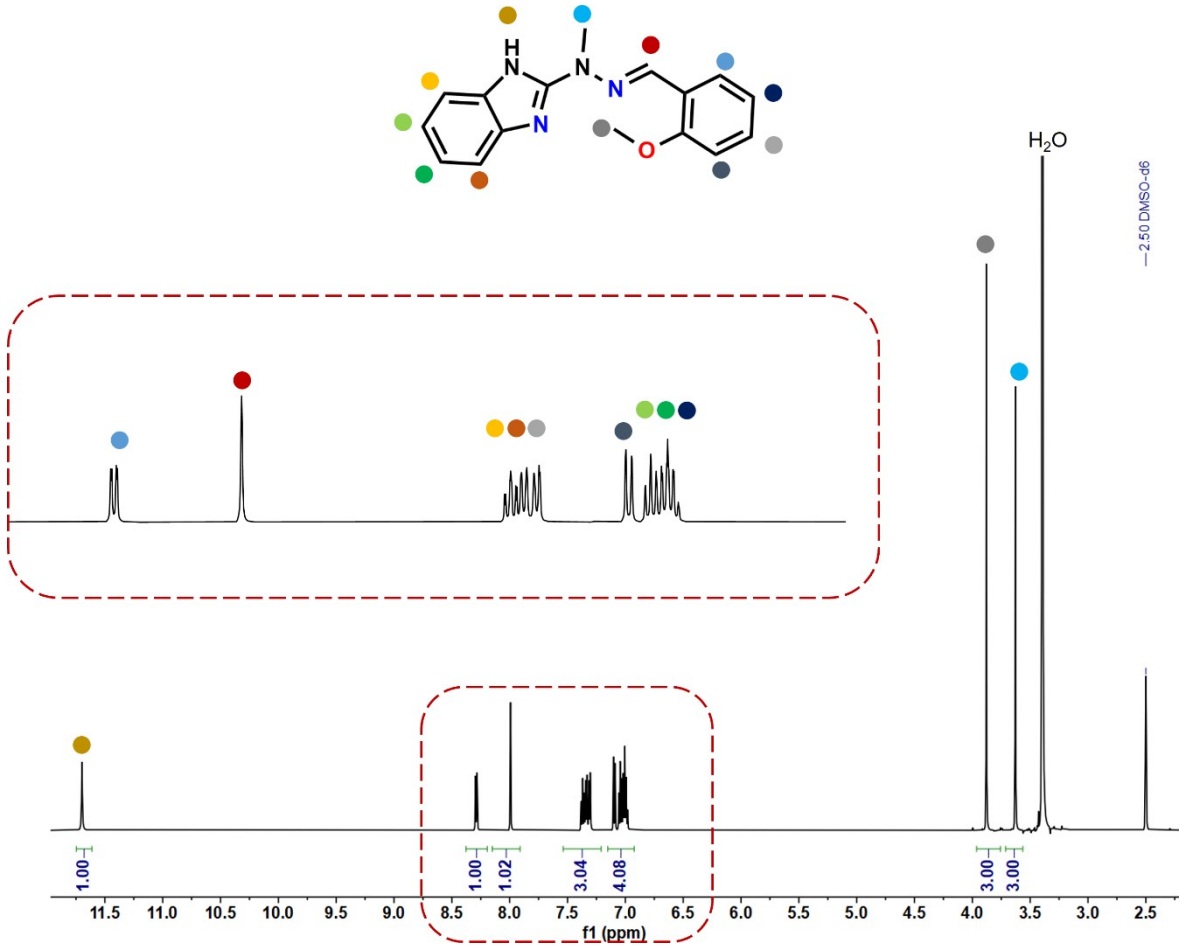

Fig. S3. ^{1}H NMR spectrum for ligand **L2** measured in $(CD_3)_2SO$.

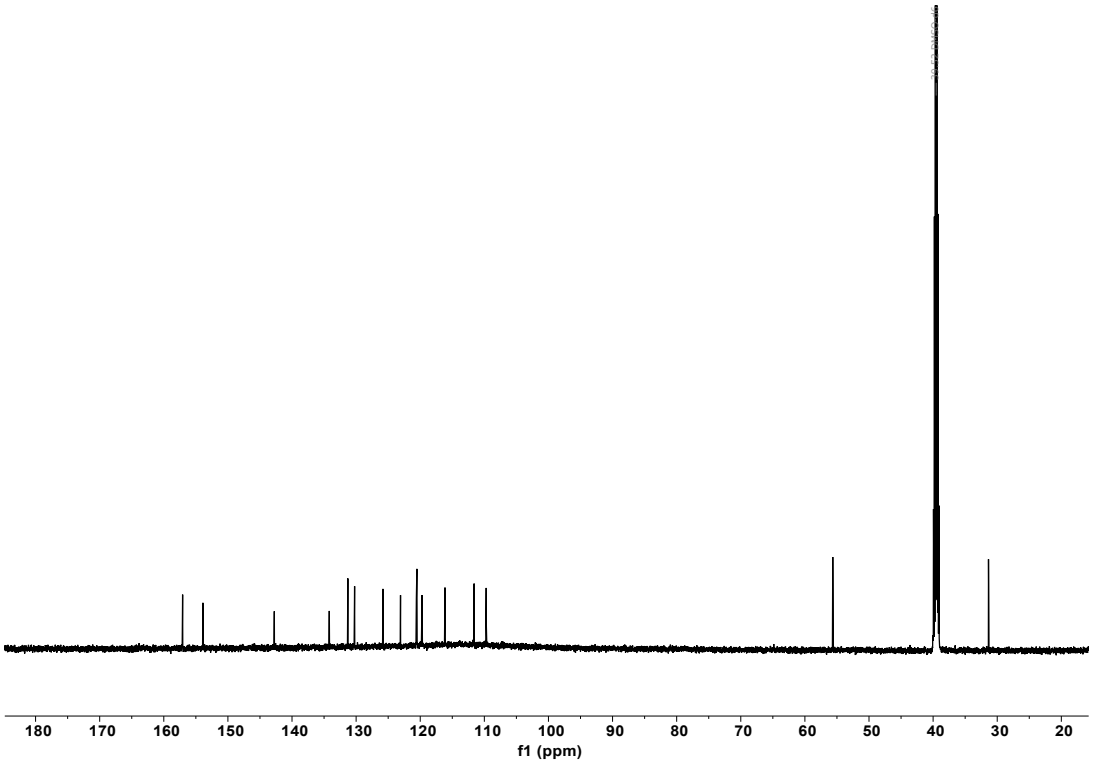

Fig. S4. ^{13}C NMR spectrum for ligand **L2** measured in $(CD_3)_2SO$.

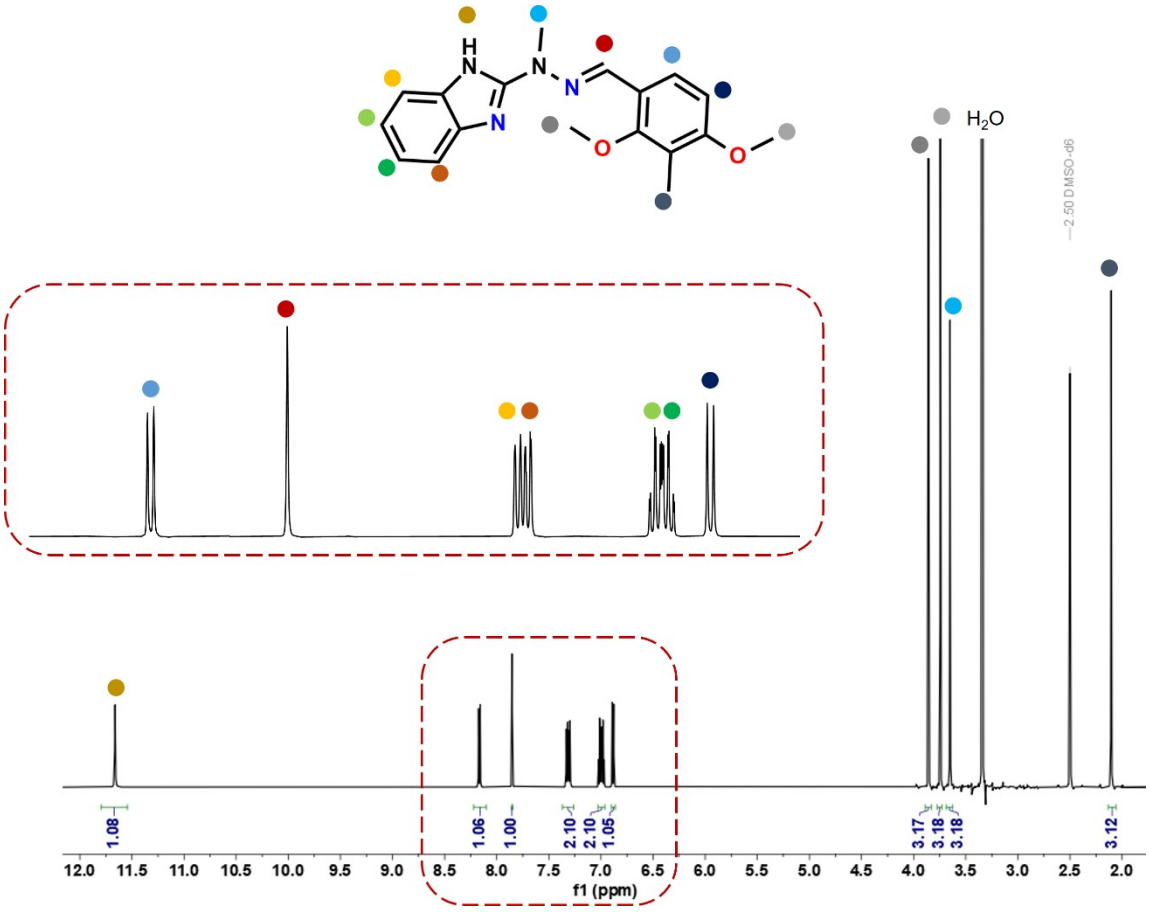

Fig. S5. ^{1}H NMR spectrum for ligand **L3** measured in $(CD_3)_2SO$.

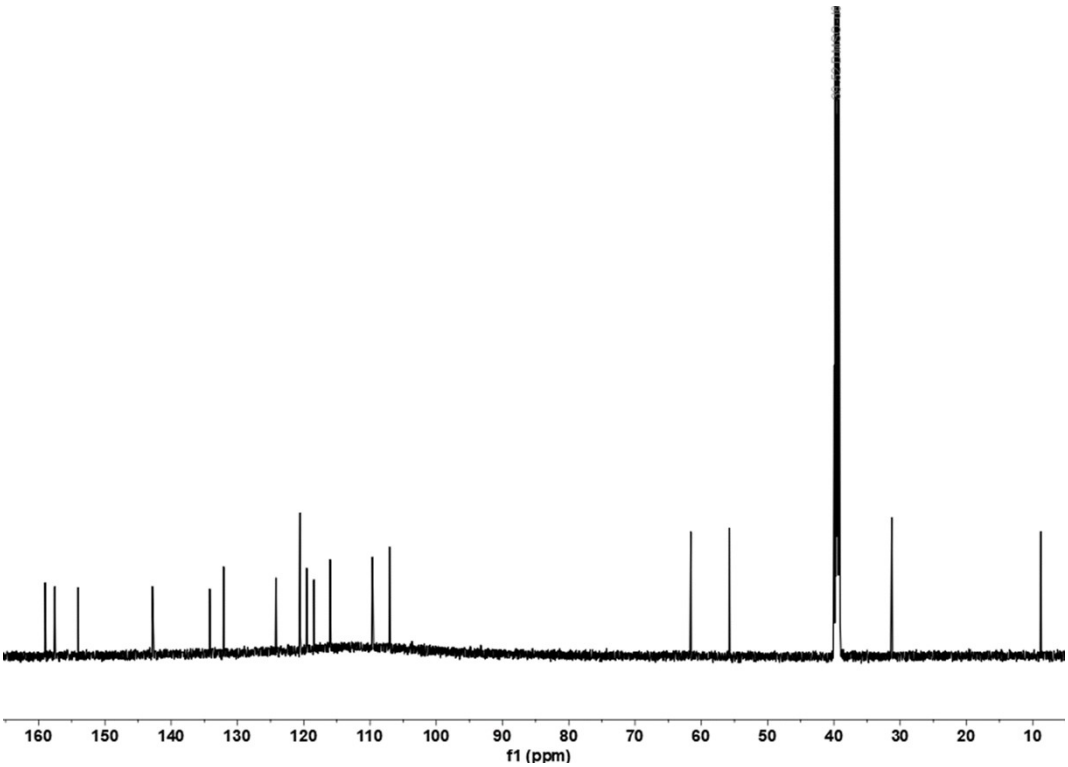

Fig. S6. ^{13}C NMR spectrum for ligand **L3** measured in $(CD_3)_2SO$.

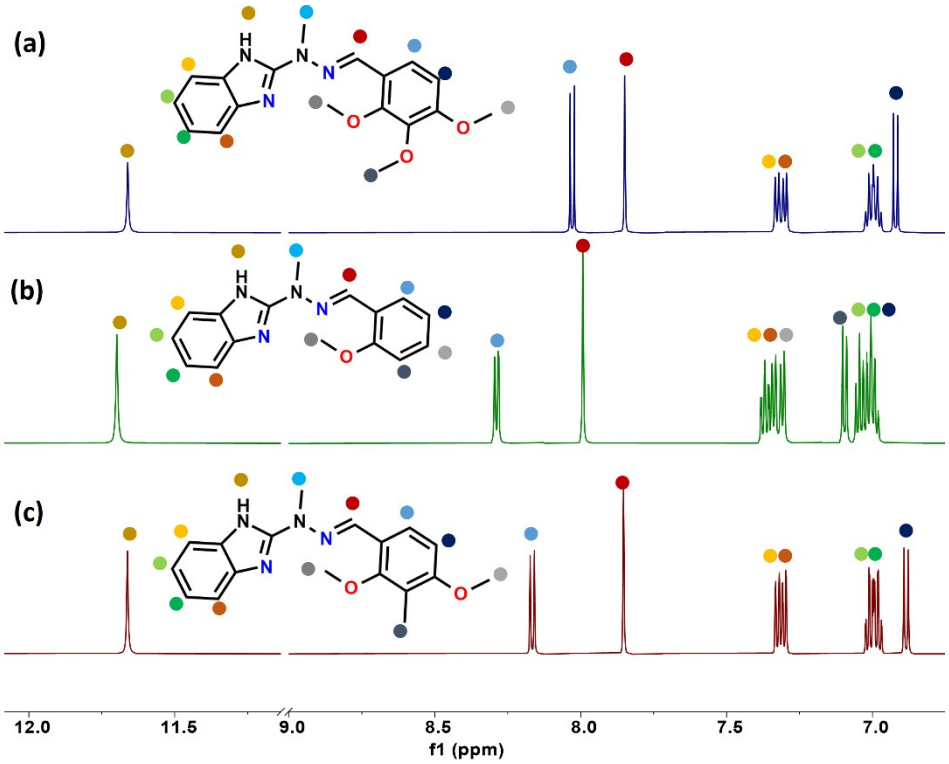

Fig. S7. Comparison of ^{1}H NMR spectra in the aromatic regions for ligands: (a) **L1**, (b) **L2** and (c) **L3** measured in $(CD_3)_2SO$.

4. IR spectra of ligand L1 – L3 and complexes C1 – C6

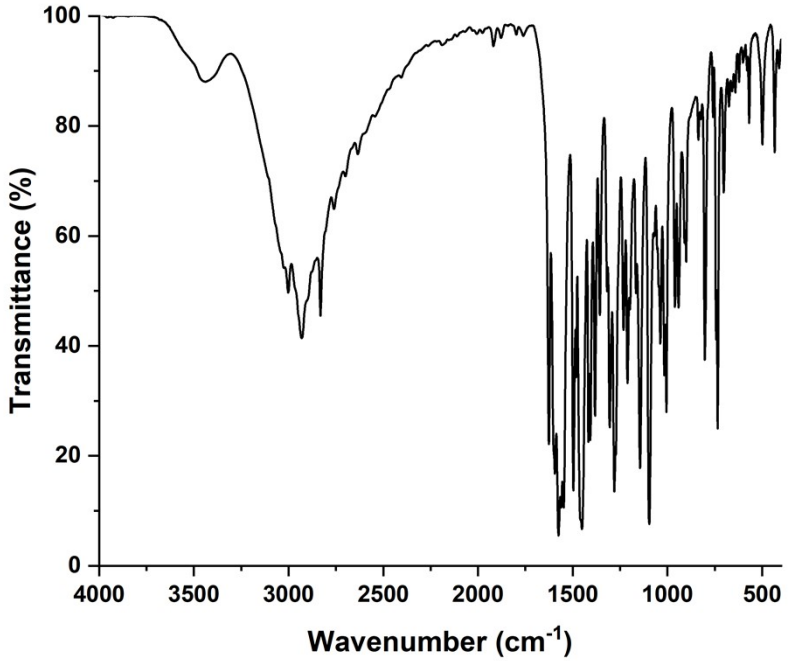

Fig. S8. IR spectrum for ligand **L1**.

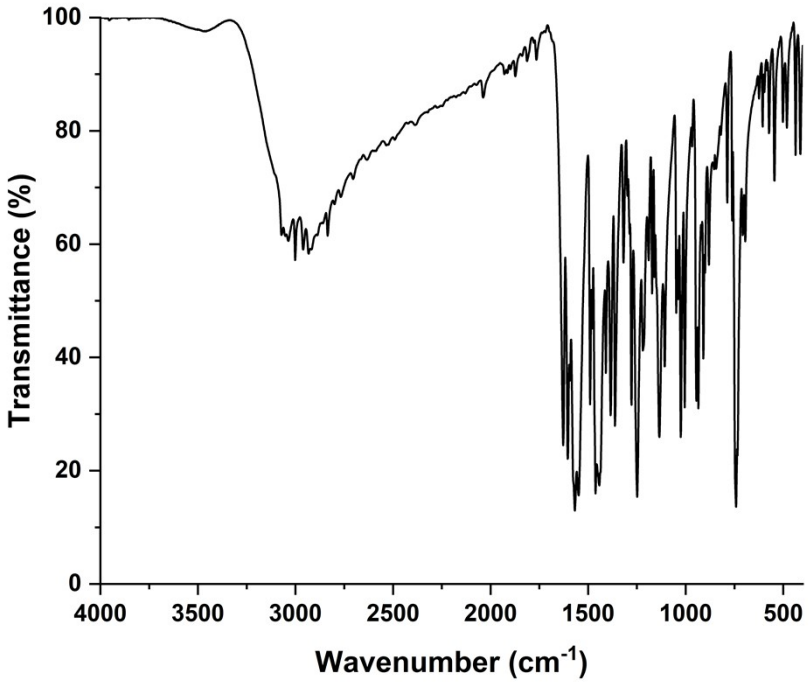

Fig. S9. IR spectrum for ligand **L2**.

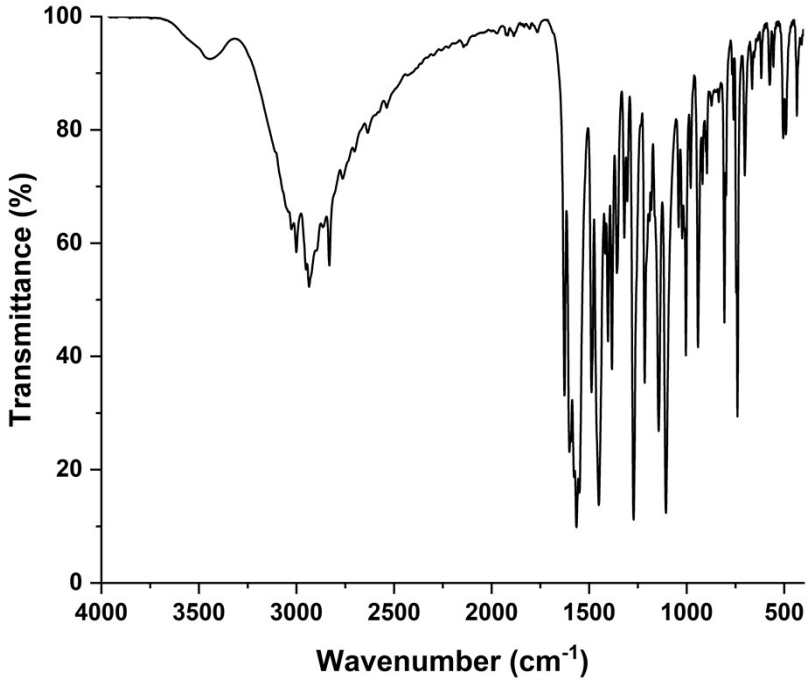

Fig. S10. IR spectrum for ligand **L3**.

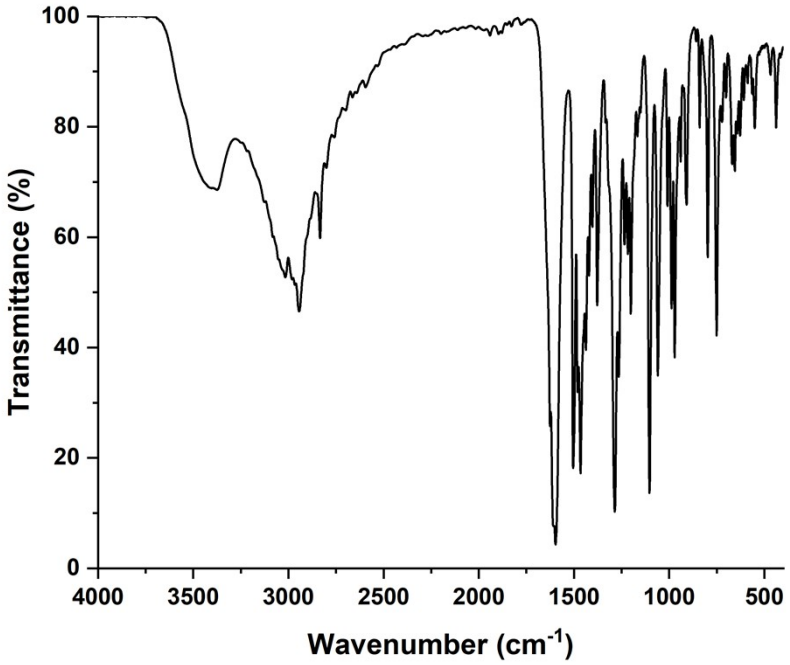

Fig. S11. IR spectrum for **C1** complex.

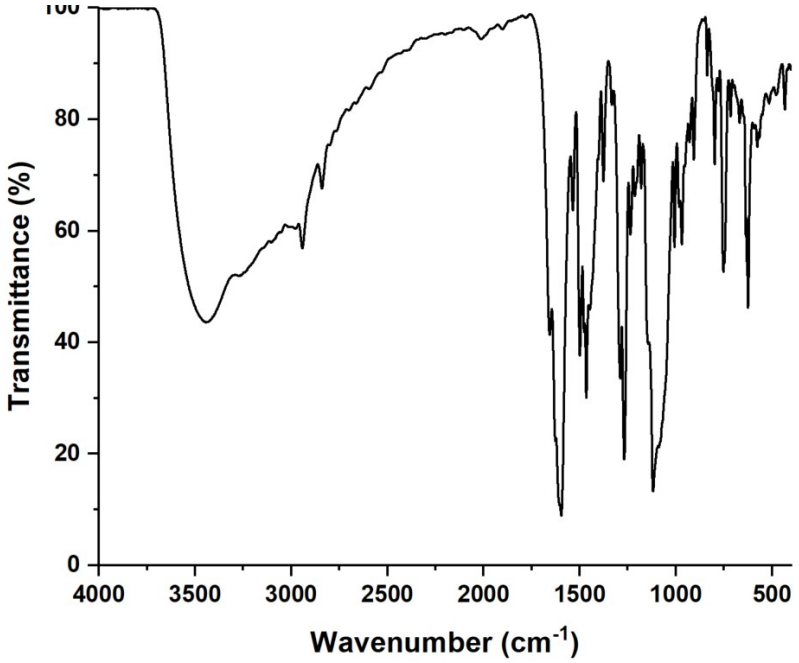

Fig. S12. IR spectrum for **C2** complex.

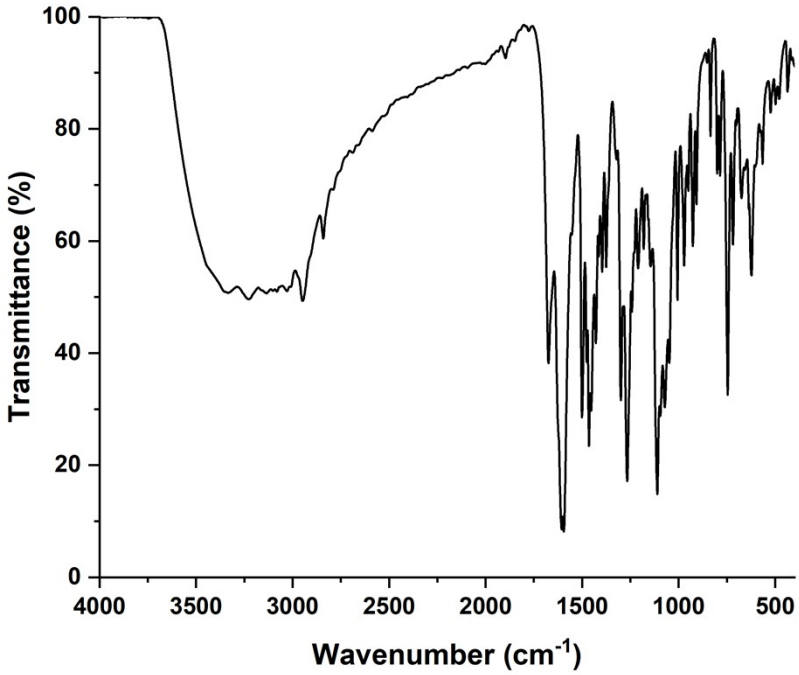

Fig. S13. IR spectrum for **C3** complex.

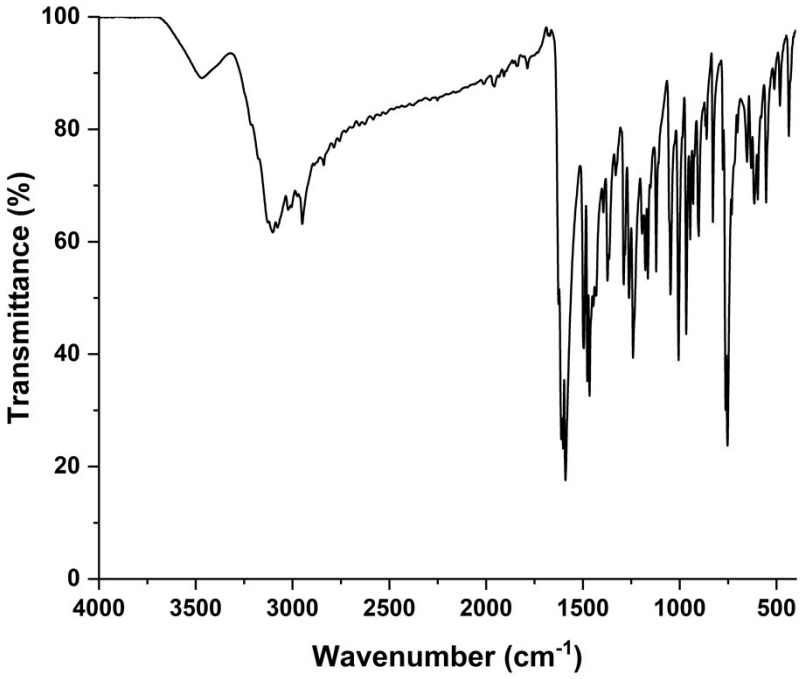

Fig. S14. IR spectrum for **C4** complex.

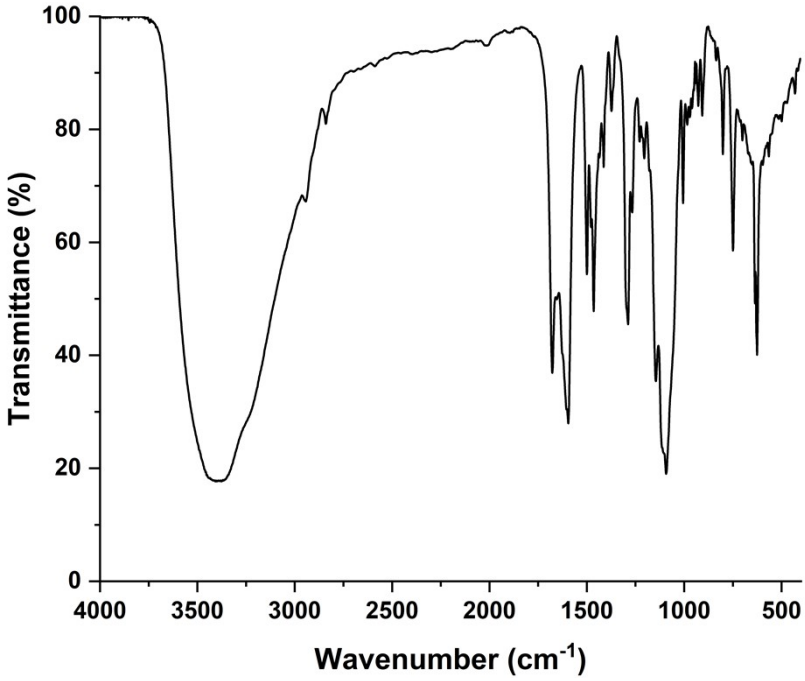

Fig. S15. IR spectrum for **C5** complex.

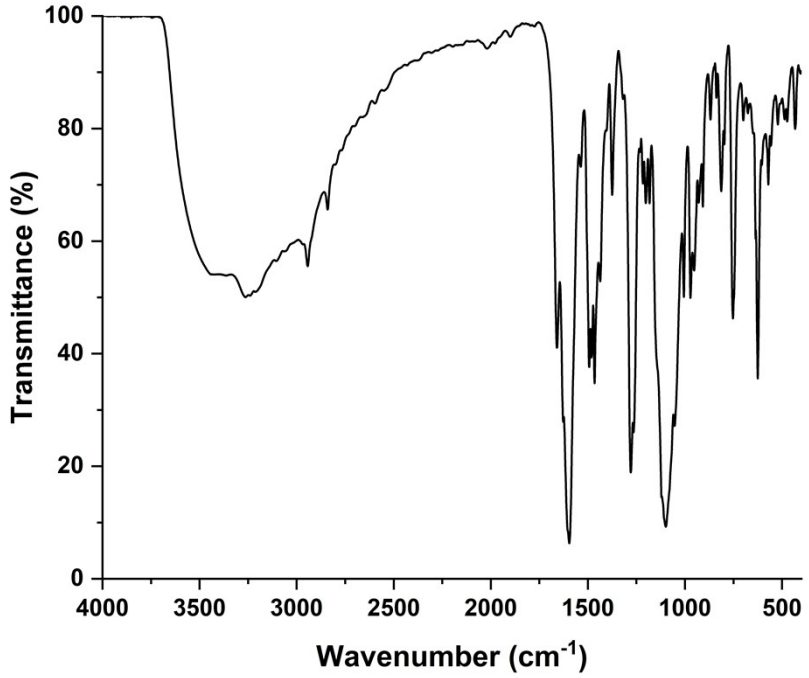

Fig. S16. IR spectrum for **C6** complex.

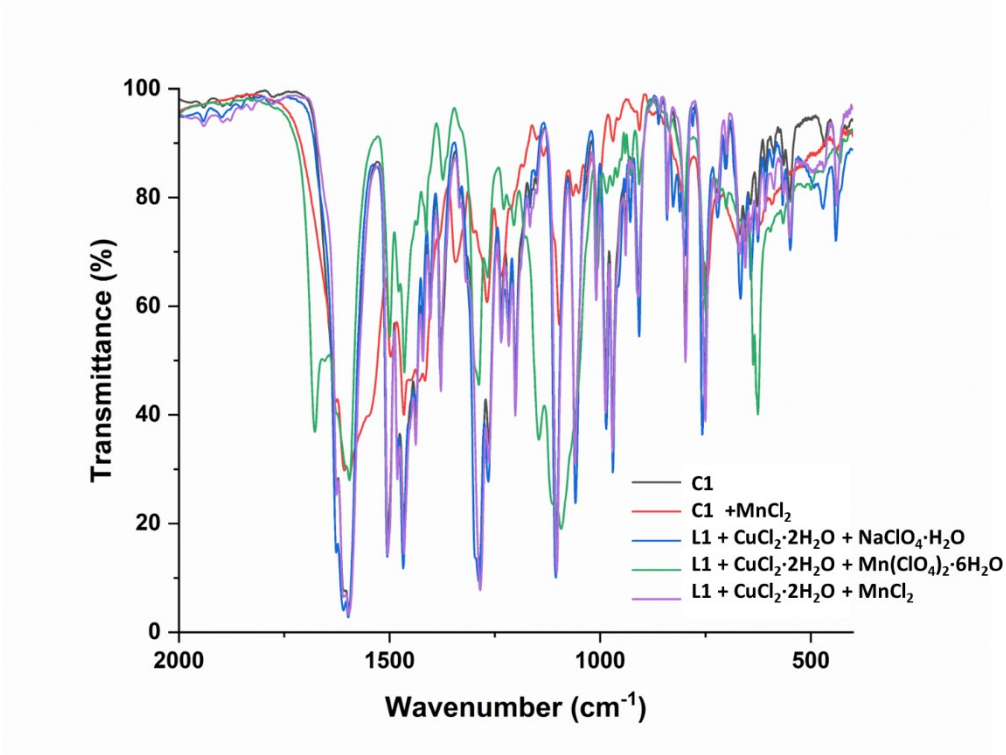

Fig. S17. Comparison of FT-IR spectra for **C1** complexes.

5. Crystallographic studies

Table S1. Crystal data, data collection and structure refinement.

Compound	**L1**	**L2**	**C2**	**C3**	**C4**	**C5**	**C6**
Formula	$C_{18}H_{21}N_4O_3^+ \cdot ClO_4^-$	$C_{16}H_{17}N_4O^+ \cdot ClO_4^-$	$C_{17}H_{17}ClCuN_4O_3$	$C_{35}H_{38}ClCu_2N_8O_{14}^+ \cdot ClO_4^- \cdot 2CH_3OH \cdot H_2O$	$C_{16}H_{16}Cl_2CuN_4O$	$C_{18}H_{20}Cl_2CuN_4O_2$	$C_{36}H_{40}Cl_2CuN_8O_8 \cdot CH_3OH$
Formula weight	440.84	380.78	424.33	1024.80	414.77	458.82	879.24
Crystal system	monoclinic	triclinic	orthorhombic	monoclinic	Triclinic	monoclinic	monoclinic
Space group	$P2_1/c$	P-1	$Pca2_1$	$P2_1/c$	P-1	$P2_1/n$	$P2_1/c$
a(Å)	13.6826(5)	7.5467(5)	18.8457(3)	16.90445(13)	8.2961(7)	14.4376(6)	12.26303(10)
b(Å)	9.7733(3)	9.9377(6)	6.69128(6)	12.18931(8)	13.6909(5)	8.0593(3)	18.89895(16)
c(Å)	15.5906(6)	11.2816(5)	13.29018(11)	22.04368(13)	14.6952(11)	16.8258(7)	17.09492(14)
α(º)	90	77.316(5)	90	90	89.989(5)	90	90
β(º)	109.453(4)	85.652(5)	90	101.9124(7)	88.450(7)	98.442(4)	97.1415(7)
γ(º)	90	88.953(5)	90	90	82.033(6)	90	90
V(Å^3)	1965.83(13)	823.06(8)	1675.91(3)	4444.36(5)	1652.4(2)	1936.59(14)	3931.15(6)
Z	4	2	4	4	4	4	4
D_x(g cm^{-3})	1.490	1.536	1.682	1.532	1.667	1.574	1.486
F(000)	920	396	868	2112	844	940	1828
μ(mm^{-1})	0.245	2.406	3.545	2.918	4.937	1.425	2.587
Reflections:							
collected	7516	6167	23536	51157	7542	7702	38953
unique (R_{int})	3932 (0.0198)	3336 (0.0313)	3492 (0.0409)	9267 (0.0337)	4997 (0.0452)	3853 (0.0295)	8136 (0.0337)
with I>2σ(I)	3295	2943	3488	8481	4500	3202	7345
R(F) [I>2σ(I)]	0.0454	0.0482	0.0258	0.0440	0.1322	0.0430	0.0469
wR(F^2) [I>2σ(I)]	0.1157	0.1368	0.0744	0.1261	0.3014	0.1121	0.1199
R(F) [all data]	0.0558	0.0532	0.0258	0.0475	0.1377	0.0539	0.0534
wR(F^2) [all data]	0.1243	0.1428	0.0744	0.1308	0.3031	0.1210	0.1243
Goodness of fit	1.051	1.097	1.078	1.022	1.002	1.038	1.027
max/min Δρ (e·Å$^-$	0.63/-0.45	0.39/-0.54	0.30/-0.43	1.00/-0.67	2.92/-1.04	0.67/-1.14	1.16/-0.45
CCDC deposition	2336936	2370349	2336938	2336939	2370350	2370351	2370352

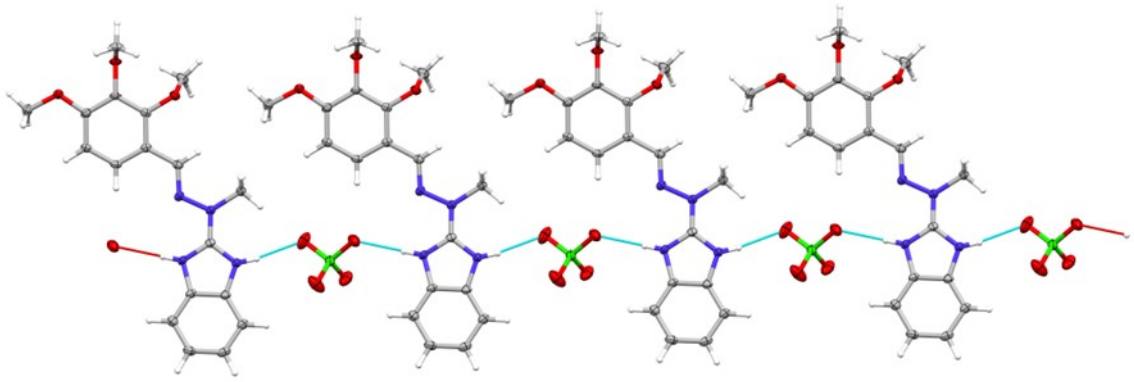

Fig. S18. Supramolecular motifs in crystal structure of ligand' salts: infinite chains (**L1**).

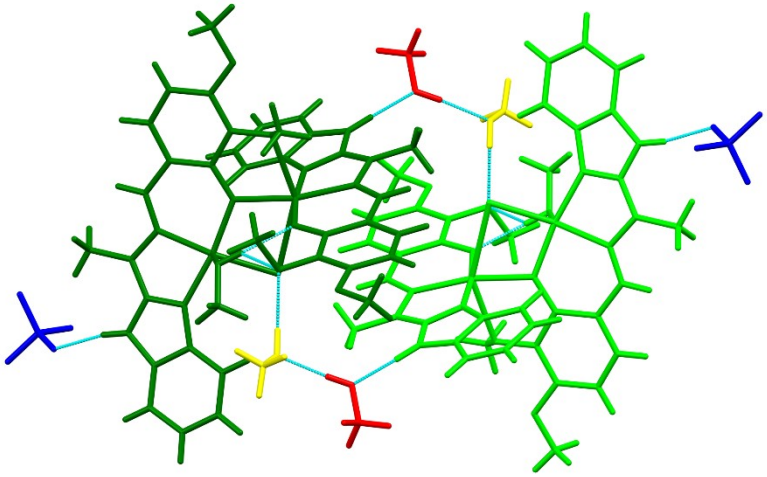

Fig. S19. Hydrogen bond system in the structure of **C3**. Dashed lines show hydrogen bonds, colour code: green – complex cations, blue – perchlorate anions, red and yellow solvent methanol molecules.

Table S2. Hydrogen bond data (Å, °) with s.u.'s in parentheses. Symmetry codes: [i] 1-x,-1/2+y,3/2-z; [ii] 1-x,1/2+y,3/2-z; [iii] x,1+y,z; [iv] -x,-1/2+y,3/2-z, [v] 1-x,1-y,1-z; [vi]1-x,1-y,2-z; [vii] 1-x,2-y,1-z; [viii] x,-1+y,z; [ix] x,3/2-y,-1/2+z.

D	H	A	D-H	H···A	D···A	D-H···A
L1						
N1	H1	O3A[i]	0.82(3)	2.18(3)	2.977(3)	163(2)
N3	H3	O2A[ii]	0.84(3)	2.19(3)	2.993(3)	161(2)
L2						
N1	H1	O4A[iii]	0.89	2.04	2.922(4)	174
N3	H3	O1A	0.88	2.03	2.855(4)	156
C2						
N3	H3	O16[iv]	0.88	1.97	2.830(2)	164
C3						
N3A	H3A	O1F[v]	0.88	1.90	2.765(4)	167
N3B	H3B	O4D	0.88	1.92	2.793(3)	169

O1C	H1C	O14A	0.84	1.96	2.776(2)	164
O1E	H1E	O15A	0.84	1.84	2.680(4)	176
O1F	H1F	O15A	0.82	2.05	2.869(3)	170
C4						
N3A	H3A	Cl2A^{vi}	0.88	2.35	3.175(5)	157
N3B	H3B	Cl1B^{vii}	0.88	2.36	3.173(5)	153
C5						
N3	H3	Cl2^{viii}	0.88	2.32	3.199(4)	178
C6						
N3A	H3A	O1D^{ix}	0.88	1.91	2.778(5)	168
N3B	H3B	O4C^{ix}	0.88	2.00	2.841(6)	153
O1D	H1D	Cl1	0.84	2.31	3.120(6)	162

Table S3. Relevant geometrical characteristics of complexes.

C2			
Cu1-N1	1.957(2)	Cu1-O14	1.885(2)
Cu1-N11	2.007(2)	Cu1-Cl1	2.2595(7)
N1-Cu1-O14	168.09(10)	N11-Cu1-Cl1	165.03(7)
C3			
Cu1A-N1A	1.9599(19)	Cu1B-N1B	1.952(2)
Cu1A-N11A	1.9911(19)	Cu1B-N11B	2.0015(19)
Cu1A- O14A	1.9215(16)	Cu1B-O14B	1.9424(16)
Cu1A-O14B	2.0188(16)	Cu1B-O1C	2.2212(17)
Cu1A-O15B	2.4051(17)	Cu1B-Cl3	2.2856(6)
Cu1A-Cl3	2.779(1)		
N1A-Cu1A-O14A	172.53(8)	N1B-Cu1B-O14B	171.71(8)
N11A-Cu1A-O14B	168.91(8)	N11B-Cu1B-Cl3	150.01(6)
O15B-Cu1A-Cl3	149.7(1)		
C4			
Cu1A-N1A	1.982(9)	Cu1B-N1B	1.973(9)
Cu1A-N11A	2.047(11)	Cu1B-N11B	2.042(11)
Cu1A-O14A	2.421(8)	Cu1B-O14B	2.427(7)
Cu1A-Cl1A	2.215(4)	Cu1B-Cl1B	2.305(3)
Cu1A-Cl2A	2.305(4)	Cu1B-Cl2B	2.208(4)
N1A-Cu1A-N11A	79.5(4)	N1B-Cu1B-N11B	79.2(4)
N1A-Cu1A-O14A	121.3(4)	N1B-Cu1B-O14B	127.6(3)
N1A-Cu1A-Cl1A	99.9(3)	N1B-Cu1B-Cl1B	130.4(3)
N1A-Cu1A-Cl2A	132.9(3)	N1B-Cu1B-Cl2B	100.7(3)
N11A-Cu1A-O14A	74.0(3)	N11B-Cu1B-O14B	75.2(3)
N11A-Cu1A-Cl1A	166.2(3)	N11B-Cu1B-Cl1B	92.8(3)
N11A-Cu1A-Cl2A	93.1(3)	N11B-Cu1B-Cl2B	166.3(3)
O14A-Cu1A-Cl1A	95.1(2)	O14B-Cu1B-Cl1B	96.0(2)
O14A-Cu1A-Cl2A	100.2(3)	O14B-Cu1B-Cl2B	94.6(2)
Cl1A-Cu1A-Cl2A	97.20(15)	Cl1B-Cu1B-Cl2B	97.40(15)
C5			
Cu1-N1	1.966(3)	Cu1-N11	2.057(2)
Cu1-O14	2.131(2)	Cu1-Cl1	2.2175(8)

Cu1-Cl2	2.4318(8)		
N1-Cu1-N11	88.08(10)	N1-Cu1-O14	146.66(9)
N1-Cu1-Cl1	100.60(7)	N1-Cu1-Cl2	115.17(7)
N11-Cu1-O14	81.95(9)	N11-Cu1-Cl1	164.65(7)
N11-Cu1-Cl2	94.88(7)	O14-Cu1-Cl1	89.75(6)
O14-Cu1-Cl2	94.11(6)	Cl1-Cu1-Cl2	98.60(3)
C6			
Cu1-N1A	1.9411(19)	Cu1-N1B	1.9325(18)
Cu1-N11A	2.2338(19)	Cu1-Cl1	2.2841(6)
Cu1-O1C	2.703	Cu1-N11B	2.552
N1A-Cu1-N11A	77.91(7)	N1A-Cu1-N1B	168.89(8)
N1A-Cu1-Cl1	97.52(6)	N11A-Cu1-N1B	92.10(7)
N11A-Cu1-Cl1	175.33(5)	N1B-Cu1-Cl1	92.54(6)
N1A-Cu1-N11B	100.2	N1A-Cu1-O1C	79.6
N11A-Cu1-N11B	75.4	N11A-Cu1-O1C	85.6
N1B-Cu1-N11B	72.3	N1B-Cu1-O1C	104.7
Cl1-Cu1-N11B	106.6	Cl1-Cu1-O1C	92.7
N11B-Cu1-O1C	160.5		

6. UV-Vis spectroscopy

The UV-Vis spectra of the ligands **L2**, **L3** and their Cu(II) complexes **C4**, **C5**, **C6** were recorded in acetonitrile at concentration equal to 0.02 mM and confirmed the stability of the complexes in solution, indicating the lack of decoordination of the imine ligands and confirming the absence of demethylated products (Fig. S20). The recorded spectra for ligands **L2**, **L3** and their complexes showed well-defined bands with maxima in the range 295 - 400 nm, which are characteristic of Cu(II) complexes with an imine bond in the ligand backbone. Moreover, for none of the compounds do we observe an additional peak at ~400 nm, characteristic of **C2** and **C3** complexes indicating changes in the ligand backbone, so we confirm the lack of formation of *O*-demethylation products for the studied compounds in acetonitrile solution.

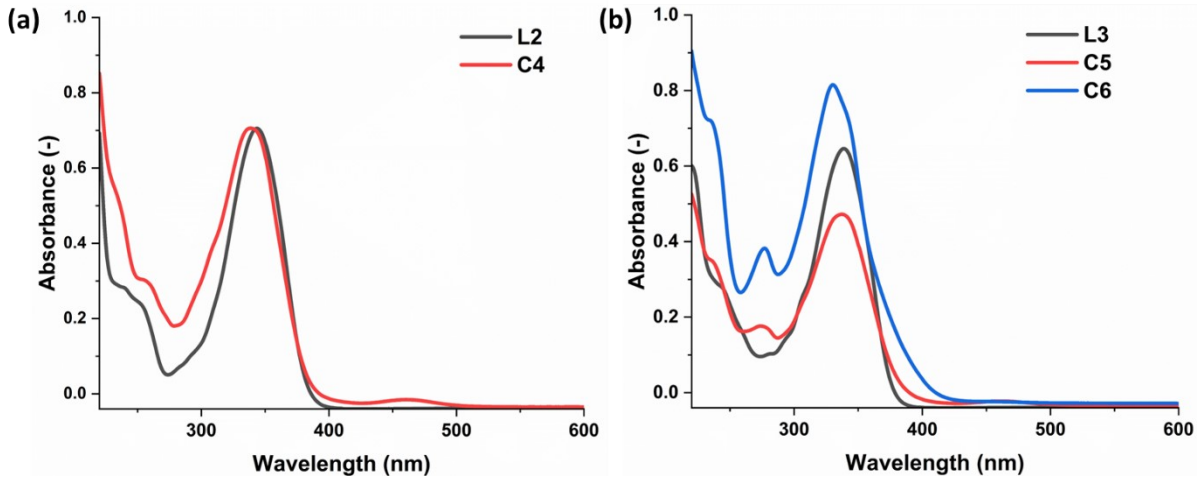

Fig. S20. (a) UV-Vis spectra of ligand **L2** and Cu(II) complex **C4** recorded in MeCN at c = 0.02 mM. (b) UV-Vis spectra of ligand **L3** and Cu(II) complexes **C5** and **C6** recorded in MeCN at c = 0.02 mM.

7. Electrochemical experiments

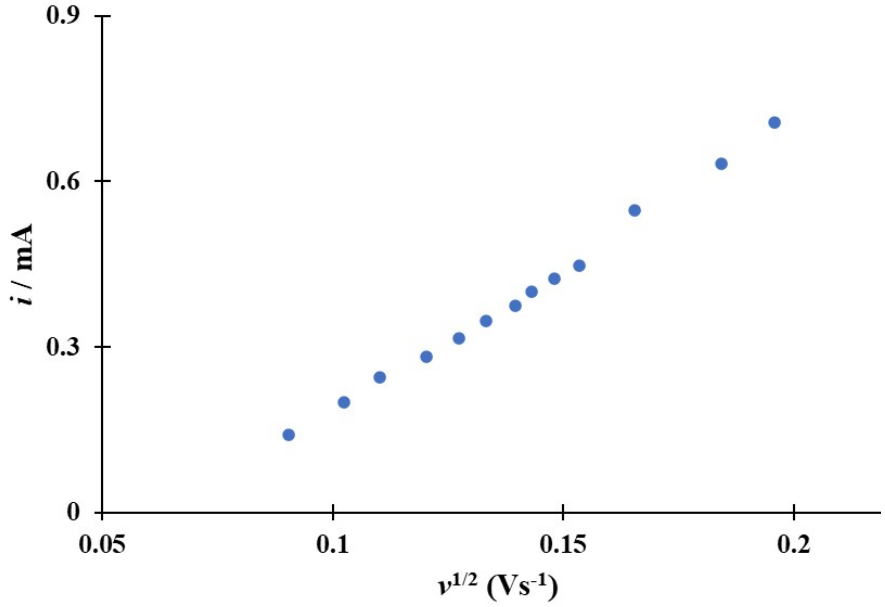

Fig. S21. The relationship between i_p and $v^{1/2}$.

8. Proposed mechanism and DFT computations

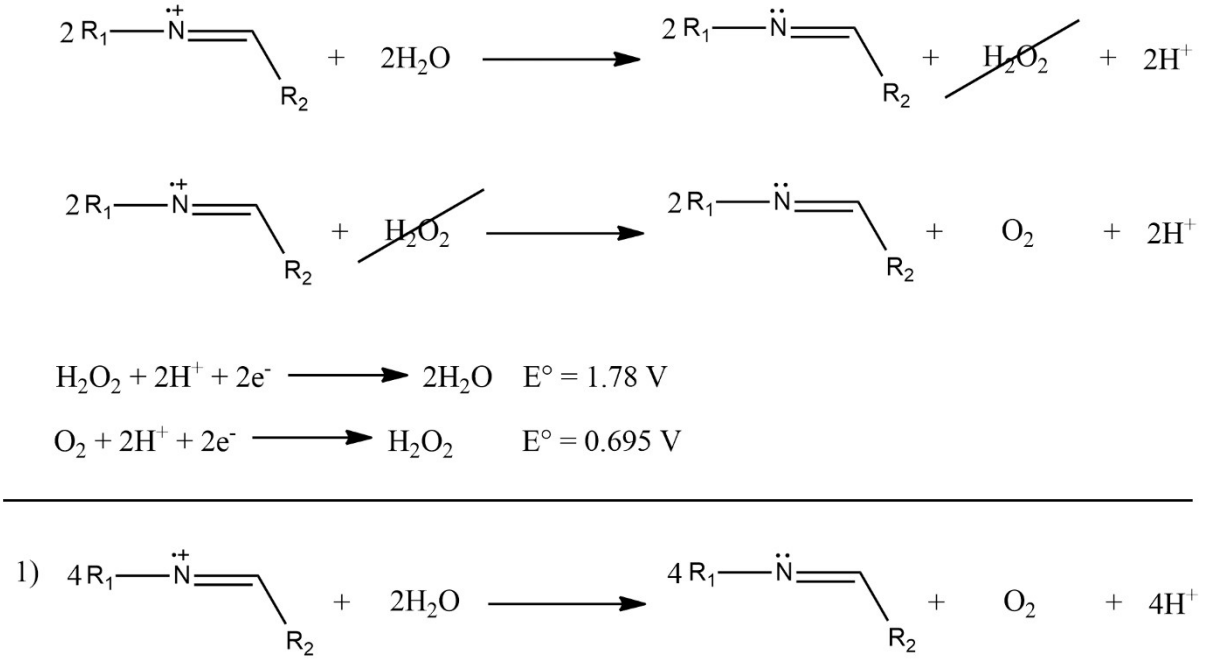

Scheme S4. Proposed reactions for the formed of hydroxide ions acting as a nucleophile in the further reaction stage.

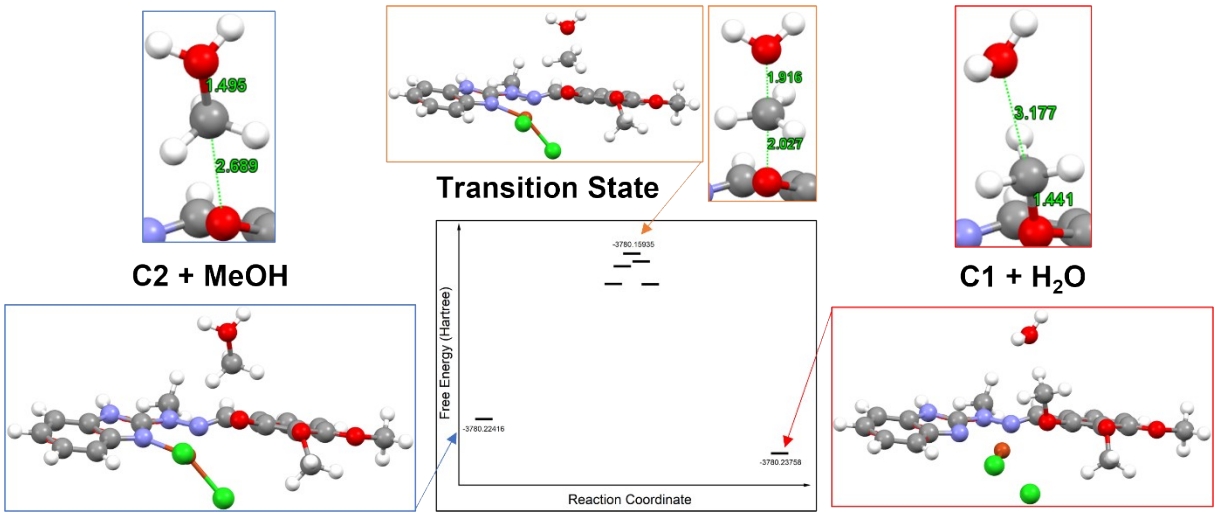

Fig. S22. Gibbs free energy profile for **C1** and the nucleophile H_2O (TS = transition state, measurement in Angstrom).

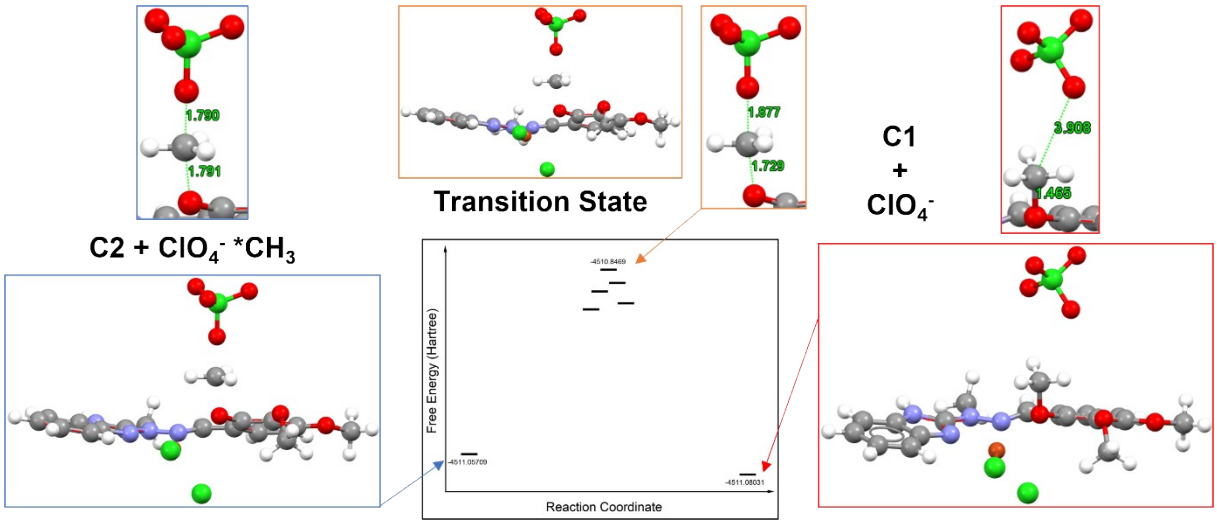

Fig. S23. Gibbs free energy profile for **C1** and the nucleophile OH^- (TS = transition state, measurement in Angstrom).